

# Modulation of Molecular Conductance Induced by Electrode Atomic Species and Interface Geometry

P. Tarakeshwar,<sup>\*,†</sup> Juan Jose Palacios,<sup>‡</sup> and Dae M. Kim<sup>†</sup>

*School of Computational Sciences, Korea Institute for Advanced Study, 207-43, Cheongyangni-2-dong, Dongdaemun-gu, Seoul 130-722, Korea, and Departamento de Física Aplicada, Universidad de Alicante, San Vicente del Raspeig, Alicante 03690, Spain*

*Received: January 18, 2006; In Final Form: February 27, 2006*

We present a systematic theoretical investigation of the interaction of an organic molecule with gold and palladium electrodes. We show that the chemical nature of the electrode elicits significant geometrical changes in the molecule. These changes, which are characteristic of the electrode atomic species and the interface geometry, are shown to occur at distances as great as 10 Å from the interface, leading to a significant modification of the inherent electronic properties of the molecule. In certain interface geometries, the highest occupied molecular orbital (HOMO) of the palladium-contacted molecule exhibits enhanced charge delocalization at the center of the molecule, compared to gold. Also, the energy gap between the conductance peak of the lowest unoccupied molecular orbital (LUMO) and the Fermi level is smaller for the case of the palladium electrode, thereby giving rise to a higher current level at a given bias than the gold-contacted molecule. These results indicate that an optimal choice of the atomic species and contact geometry could lead to significantly enhanced conductance of molecular devices and could serve as a viable alternative to molecular derivatization.

## Introduction

A major factor impeding the fabrication of high-performance molecular electronic devices is the limited understanding of the role of the electrode in the overall device performance.<sup>1–4</sup> The difficulties in understanding the interface problem stem from the fact that a molecule with a series of discrete states is in contact with a bulk electrode with a dense set of states.<sup>2,3</sup> The difficulty is compounded by the absence of reliable experimental methods to determine the detailed atomic structure of the electrode–molecule system and its influence on the electron-transport properties of the molecule. Despite these problems, a number of theoretical studies have provided insights regarding the role of both the electrode and the contact geometry in modulating the electrical characteristics of the molecule.<sup>1–11</sup>

Most of these studies have focused on the nature of bonding between the molecule and the electrode and on the charge transfer between the two at zero bias, based on the alignment of molecular orbitals' energy levels with respect to the Fermi energy of the electrode.<sup>1,5–11</sup> However, an important but overlooked consideration is the role of the chemical nature of the electrode in affecting the structure and inherent electronic properties of the molecule. The few studies that have addressed this issue have been confined to charge effects occurring at the interface. This is rather surprising given the fact that most of the molecules exhibiting promise as potential electronic devices are conjugated systems.

A great deal of experimental and theoretical evidence in the fields of the organometallic chemistry and nonlinear optical materials indicates that the insertion of a metal unit into a conjugated structure significantly alters the  $\pi$ -electron behavior of the molecule.<sup>12,13</sup> Recent work carried out by us on carbon

nanotubes contacted with different metal electrodes also indicates that the electronic characteristics of the carbon nanotubes are significantly modulated by the metal electrode.<sup>14,15</sup> Specifically, our study showed that metal electrodes having very similar work functions can give rise to rather different effects on the electronic characteristics of the nanotubes. Therefore, it is interesting and relevant to examine the role of the chemical nature of the electrode in influencing the electronic characteristics of smaller molecules. In addition, we examine the effects of the geometric configuration of the electrode–molecule interface and analyze its role in modulating the electrical characteristics of the molecule. Finally, an assessment is made as to whether changing the chemical nature of the electrode could be an alternative to existing methods of modulating the electrical characteristics of a molecule, viz., molecular derivatization.<sup>16</sup>

To date, most detailed investigations of the effect of electrodes have been limited to small molecular systems such as benzenethiols.<sup>7–9</sup> Thus, we felt that a larger molecular system would be more appropriate to examine the role of changing the electrodes. The anthracene derivative A (Figure 1) that was experimentally investigated by Reichert et al. is particularly well suited for this investigation.<sup>17</sup> This nearly ~2-nm-long molecular system, composed of two phenyl rings coupled to a central anthranyl ring by a triple-bonded carbon bridge, was theoretically investigated by Heurich et al.<sup>18</sup> However, in their study, the transport characteristics were reported for the simple case of an isolated molecule contacted to single gold atom. In the present work, we have comprehensively examined the electronic and transport characteristics of A by considering: (i) different atomic species for the electrode, viz., gold and palladium, having nearly identical work functions and (ii) different geometric configurations by which the electrode atoms are interfaced with the molecule. These two considerations will shed insights regarding the genuine chemical nature of the molecule—

\* To whom correspondence should be addressed. E-mail: tara@kias.re.kr.

<sup>†</sup> Korea Institute for Advanced Study.

<sup>‡</sup> Universidad de Alicante.

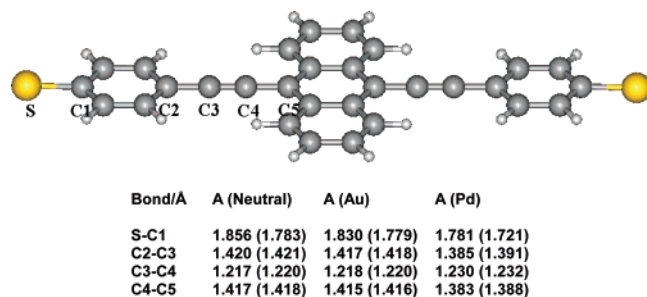


**Figure 1.** Structure of the symmetric molecule A. The lengths of a few bonds and their modulation in the corresponding Au- and Pd-contacted systems are also shown. The first values listed were obtained at the B3LYP/3-21G level, whereas those in parentheses were obtained at the B3LYP/6-31G\* level.

electrode interface and will also provide useful guidelines for fabricating molecular devices. The choice of a palladium atom was also dictated by the fact that, in contrast to metals such as titanium and aluminum,<sup>19</sup> palladium does not react with oxygen at normal temperatures.<sup>20</sup>

### Computational Details

The electronic structure calculations were carried out at the density functional level employing Becke's three-parameter functional with the Lee–Yang–Parr correlation (B3LYP). The geometries of the isolated molecules and those with different electrodes were fully optimized using the 3-21G and 6-31G\* basis sets for the carbon, hydrogen, and sulfur atoms.<sup>21</sup> The metal atoms were represented by the CRENBS and LANL2DZ basis sets.<sup>22,23</sup> In these metal basis sets, the core electrons are replaced by effective core potentials (ECPs).

A critical issue in the calculation of transport characteristics is the representation of the atomic structure of the interface. Because the actual atomic structure is unknown and is prone to change from sample to sample under identical processing, we carried out calculations using finite ensembles of metal atoms to represent the metal electrode. This approach has some limitations because of plausible differences in structures in comparison to extended metal electrode systems. However, it has previously been shown that theoretical calculations employing quantum-chemical cluster methods provide an accurate description of the interactions prevailing at metal–molecule interfaces.<sup>24</sup>

Given the uncertainty involved in predicting (i) the broadening of molecular orbitals due to coupling with the electrodes and (ii) the positioning of the Fermi level with respect to the HOMO and LUMO of the molecule, it is imperative to carry out transport calculations using ab initio methodologies.<sup>11,25–27</sup> Apart from facilitating a quantitative comparison with experiment, transmission results from ab initio calculations enable one to obtain insight into the role of the individual molecular orbitals.

Ab initio transport calculations have generally been based on the Landauer formalism, wherein the zero-bias, zero-temperature conductance is proportional to the quantum mechanical transmission probability for the electrons at the Fermi energy,  $E_F$ , to be transported across the molecule. In computational terms, the transport calculation involves the evaluation of either the scattering wave functions or the Green functions.

In a detailed formalism outlined by one of us, it was shown that the self-consistent Hamiltonian and Fock matrices obtained from a standard self-consistent-field (SCF) calculation of the molecule and a significant part of the electrodes could be employed to evaluate the ab initio transmission characteristics of the molecule.<sup>26,27</sup> Crucial to the above formalism is a simple and elegant incorporation of the infinite electrodes in the calculation. In particular, the bulk electrodes are represented using a parametrized tight-binding Bethe lattice model with the coordination number and effective parameters appropriate for the type of electrodes. The advantage of the Bethe lattice is that it provides a fair representation of the bulk density of states and the polycrystalline nature of the electrodes. The latter is possible because the Bethe lattice does not present long-range order while retaining short-range order.<sup>26–27</sup>

The evaluation of the current  $I$  involves the evaluation of the Hamiltonian and the Fock matrix for every value of the bias  $V$ . All transmission and  $I$ – $V$  calculations were performed with the package ALACANT (Alicante Ab initio Computation Applied to Nanotransport) interfaced with Gaussian 03. More details about the methodology of transmission and current calculations can be obtained from a few representative publications.<sup>26–28</sup>

### Results and Discussion

The presence of a triple-bonded carbon bridge between the central anthracene and terminal phenyl rings is one of the prominent geometrical features of A.<sup>17</sup> It was shown earlier that

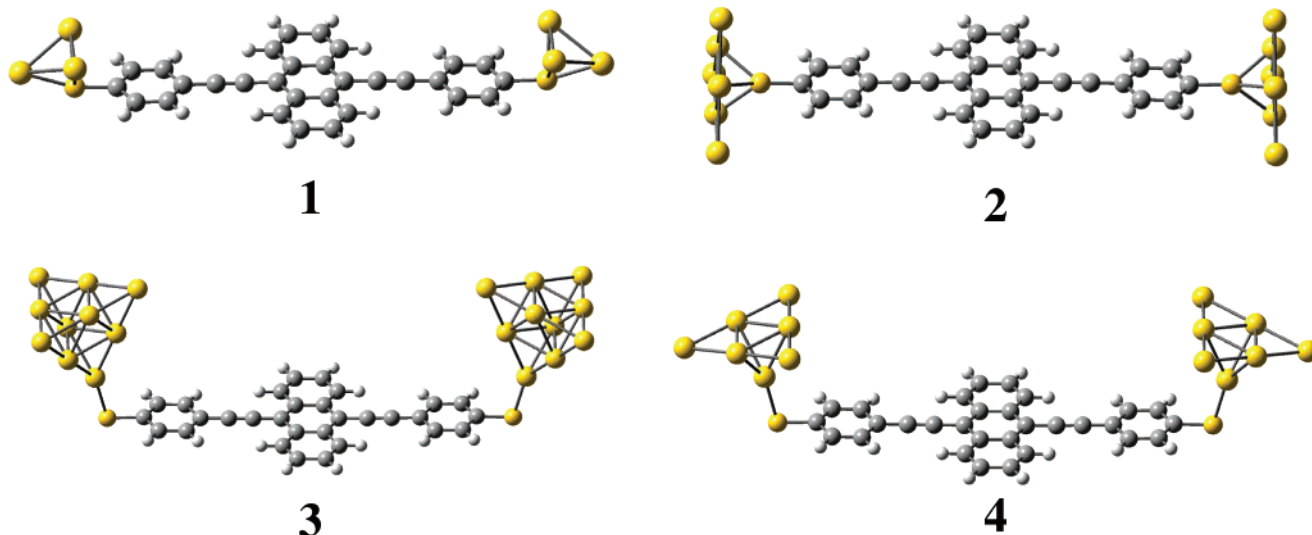


**Figure 2.** Structures of the various electrode–molecule configurations investigated in this study. For the sake of brevity, only the gold-contacted conformers are shown.

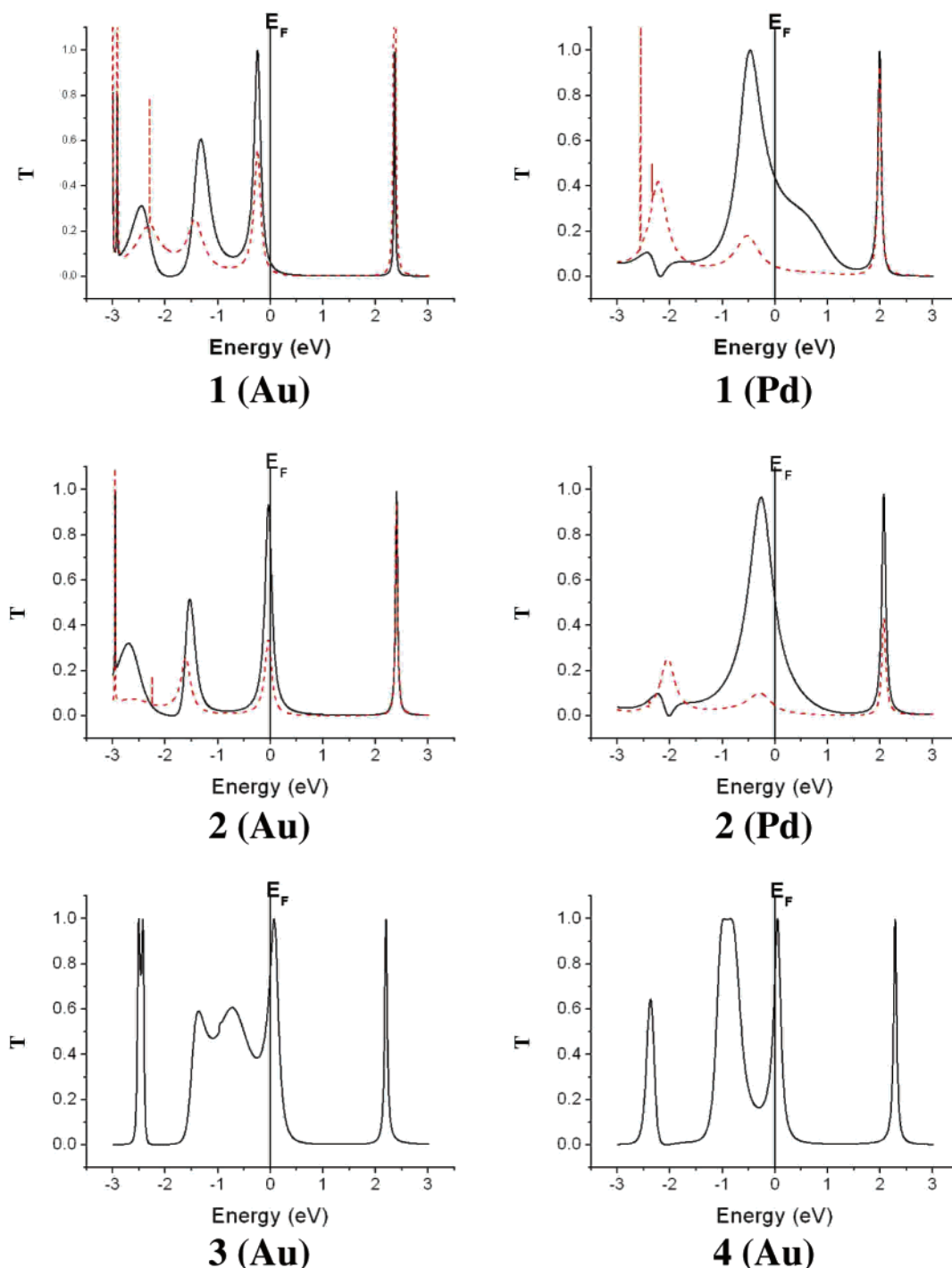


**Figure 3.** Transmission curves of all of the Au- and Pd-contacted systems (1–4) investigated in this study. The corresponding DOS of systems 1 and 2 are shown as dotted lines.

molecular transmission is mediated through orbitals involving the terminal phenyl rings, the connecting triple bonds, and the central anthranlyl ring. Therefore, changes occurring in the geometrical features of any of these can affect the transmission.<sup>18</sup> In particular, changes in the geometrical features of the triple bond enable one to obtain a reliable estimation of the extent of electronic modification induced by the electrode.

An initial geometry optimization of **A** put into contact with a single gold or palladium atom on each side indicated that contact with palladium significantly increases the length of the triple bond (Figure 1). This is accompanied by a concomitant decrease in the length of the single bond connecting the triple-bonded carbon bridge to the two rings. In contrast, the gold-

contacted **A** did not display any geometrical differences when compared to isolated **A** except for the terminal S–C bonds. Whereas geometrical changes in the S–C1 bond length can be anticipated in view of the electrode metal atom being directly bonded to the sulfur atom, the modulation of the triple-bonded C3–C4 is particularly interesting. This is because the effect has to be mediated through an intermediary phenyl ring. The geometrical changes in the triple bond and the adjacent single bonds imply that the charge localized on the triple bond is getting delocalized over the neighboring single bonds in the palladium-contacted **A**.

The improved delocalization in the palladium-contacted **A** results in a B3LYP/6-31G\* HOMO–LUMO gap of 0.6 eV, as



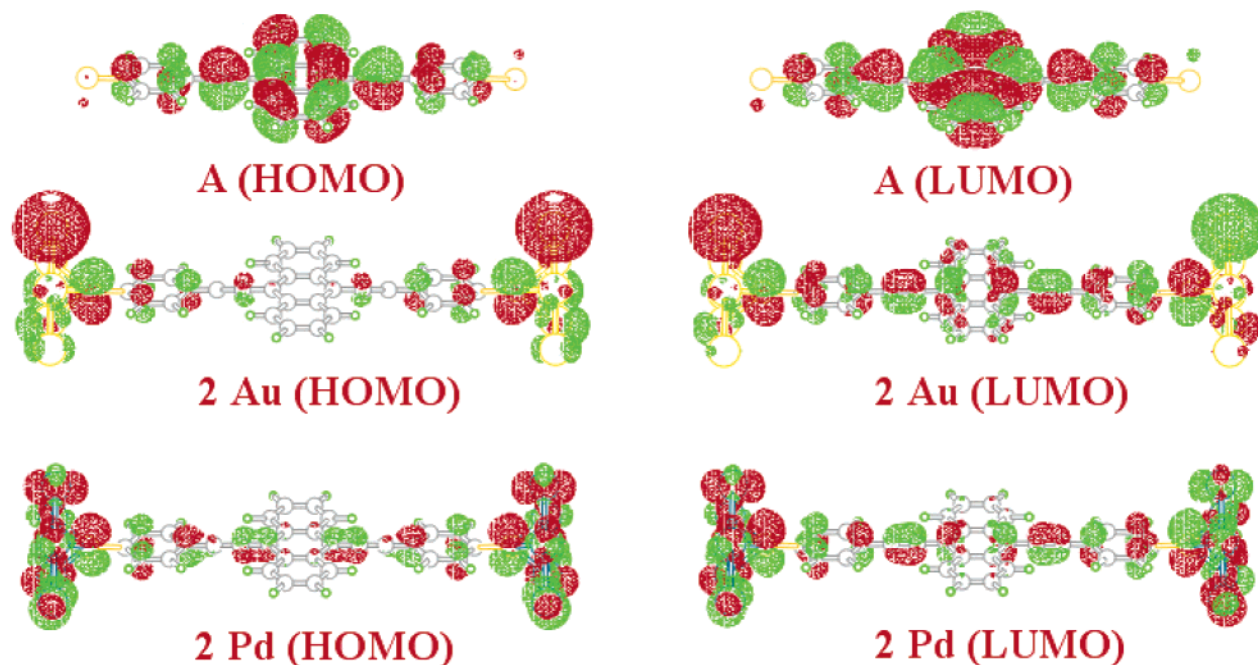


**Figure 4.** Comparison of the HOMOs and LUMOs of neutral molecule A, the Au-contacted system (2Au) and the Pd-contacted system (2Pd).

compared to the corresponding gap of 1.7 eV in gold-contacted A. Also, the LUMO of the gold-contacted A is about 0.4 eV higher in energy than that of the palladium-contacted A. These results entail a significant difference in the transport characteristics of the gold- and palladium-contacted molecules, as will be elaborated later.

Interestingly, the palladium atom lies in the plane of the molecule, whereas the gold atom lies in a plane perpendicular to the molecule in the optimized geometries of the electrode. As will be shown later, this has a significant bearing on the optimization of the cluster geometries. As both the B3LYP/3-21G and B3LYP/6-31G\* calculations yield similar differences, we restrict ourselves to results obtained at the B3LYP/3-21G level for the larger systems.

Similar geometrical changes were observed when the terminal electrode atoms were substituted with small metal clusters (structures 1 and 2, Figure 2). In optimizations involving these metal clusters, the electrode atoms (obtained from the corresponding 111 geometries) were kept at fixed positions. Incidentally, both structures 1 and 2 correspond to the energetically most favorable binding of the molecule to the three-atom hollow site of the electrode.

In an effort to examine other electrode configurations, we carried out calculations on structures 3 and 4 (Figure 2). In both of these conformations, the sulfur atom is bonded to a single atom of the metal electrode (on-top binding). Whereas the conformations corresponding to the gold-contacted molecule could be optimized, the corresponding palladium-contacted systems could not be optimized. Therefore, the transmission and  $I$ - $V$  characteristics of only the optimized gold-contacted 3 and 4 structures have been evaluated.

The zero-bias transmission curves of both the gold- and palladium-contacted 1 and 2, shown in Figure 3, exhibit a prominent conductance peak near the Fermi level. This conductance peak is associated with the HOMO in both 1 and 2, as indicated by Mulliken population analysis, revealing a small amount of charge transfer from the molecule to the electrode. This charge transfer is expected because the chemical potentials of the isolated leads are lower than the Fermi energy of the

molecule. For palladium-contacted 1 and 2 there is no discernible transmission from any other HOMO. However, other small transmissions are contributed by additional occupied molecular orbitals in the case of the gold-contacted 1 and 2. It can also be noted that the conductance peak near the Fermi level is much broader for palladium-contacted 1 and 2, indicating a strong coupling between the molecule and the electrode. This will be further elaborated in conjunction with molecular orbitals.

Apart from the broadening of the conductance peaks, the change in the position of the metal electrode with respect to the molecular plane is shown to lead to the shifting of the HOMO conductance peak closer to the Fermi level. This shift, which is independent of the chemical nature of the electrode, mirrors the shifts in the energies of the HOMOs of the gold- and palladium-contacted 1 and 2. It is also pointed out that the conductance peaks and the corresponding density of states (DOS) in Figure 3 clearly indicate the contribution of only one LUMO. This is in contrast to the previous result in which two unoccupied molecular orbitals were shown to contribute to the conductance.<sup>18</sup>

A highlight of Figure 3 is the location of the peaks of LUMO transmission and corresponding DOS relative to the Fermi level. Specifically, those peaks are shown to appear at  $\sim 2.5$  and  $\sim 2.0$  eV above the Fermi level in the case of gold and palladium contacts, respectively. Obviously, this will induce different output currents for given input voltages. Transmission calculations performed on different electrode orientations of gold (structures 3 and 4, Figure 3) indicate that the LUMO conductance peak appears at nearly the same energies. It can be argued that the use of different density functional methods might affect the peak locations. However, the use of the B3LYP functional is believed to circumvent most of the problems encountered in calculations carried out using the local density approximation (LDA). In particular, the partial removal of the self-interaction problem due to the presence of nonlocal exchange in B3LYP is important when the charge localization is strong (as is the case here). One consequence is the separation of peaks and concomitant reduction of the off-resonance

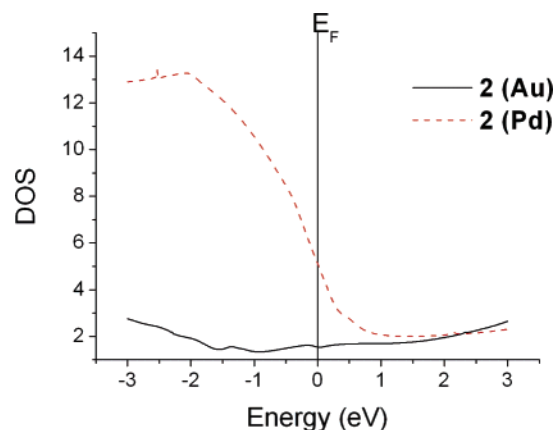


**Figure 5.** Comparison of the density of states (DOS) projected at the tip of the electrode atoms in both the Au-contacted system (2Au) and the Pd-contacted system (2Pd).

conductance compared to results obtained using either the LDA or generalized gradient approximation (GGA) methods.<sup>25</sup>

In Figure 4, we compare the characteristics of the HOMOs and LUMOs of both the gold- and palladium-contacted **2** with that of the neutral molecule **A**. Clearly, the HOMO and LUMO of isolated **A** are characterized by a marked absence of electron density on the sulfur atom. Interestingly, the HOMO of isolated **A** is very similar to the HOMO of **A** in contact with the single gold atom.<sup>18</sup> The coupling of **A** with the electrode atoms is indeed shown to induce marked changes in the characteristics of both the HOMO and LUMO of **A**. The HOMO and LUMO of the gold- and palladium-contacted **2** look similar, but interesting differences exist between them. First, the electron density tends to be more delocalized, extending to the center

of the molecule in the case of the latter. As mentioned earlier, this electron delocalization results in the palladium-contacted LUMO appearing at a lower energy than the gold-contacted LUMO. Additionally, the extent of overlap at the electrode–molecule interface is more pronounced in case of the palladium-contacted **A**. A similar observation can be made in case of the HOMOs, which, in turn, explains the observed broadening of the HOMO conductance peaks in the case of the palladium-contacted system.

The differences in the orbital overlap of the metal and sulfur atoms in the gold- and palladium-contacted systems can be attributed both to the characteristics of the metal frontier orbitals (spherically symmetric 6s orbital in case of Au, directional 4d orbitals in case of Pd) and to the corresponding orbital energies. In addition to the enhanced overlap at the interface, the DOS of the palladium-contacted molecule is much larger than that of the gold-contacted molecule (Figure 5). The basic chemical bonding inherent at the contact interface, together with the ensuing electronic effects, influences the *I*–*V* characteristics of these systems, as can be seen from Figure 6.

In discussing the calculated *I*–*V* curves, it is noted at the outset that most theoretical studies involving density functional methods could overestimate the measured current by several orders of magnitude.<sup>6–11,18,26–28</sup> Furthermore, it was very recently pointed out that wide variations can also be observed in experimental measurements of the conductance of molecular junctions.<sup>29</sup> However, in the context of this investigation, our calculations also overestimate the measured data by a factor of about 40.<sup>17</sup> To reduce this discrepancy, it is important to examine the approximations entailed in the density functional methods, in connection with the density of states factors and transmission curves especially under biases. Also, the nature and atomic

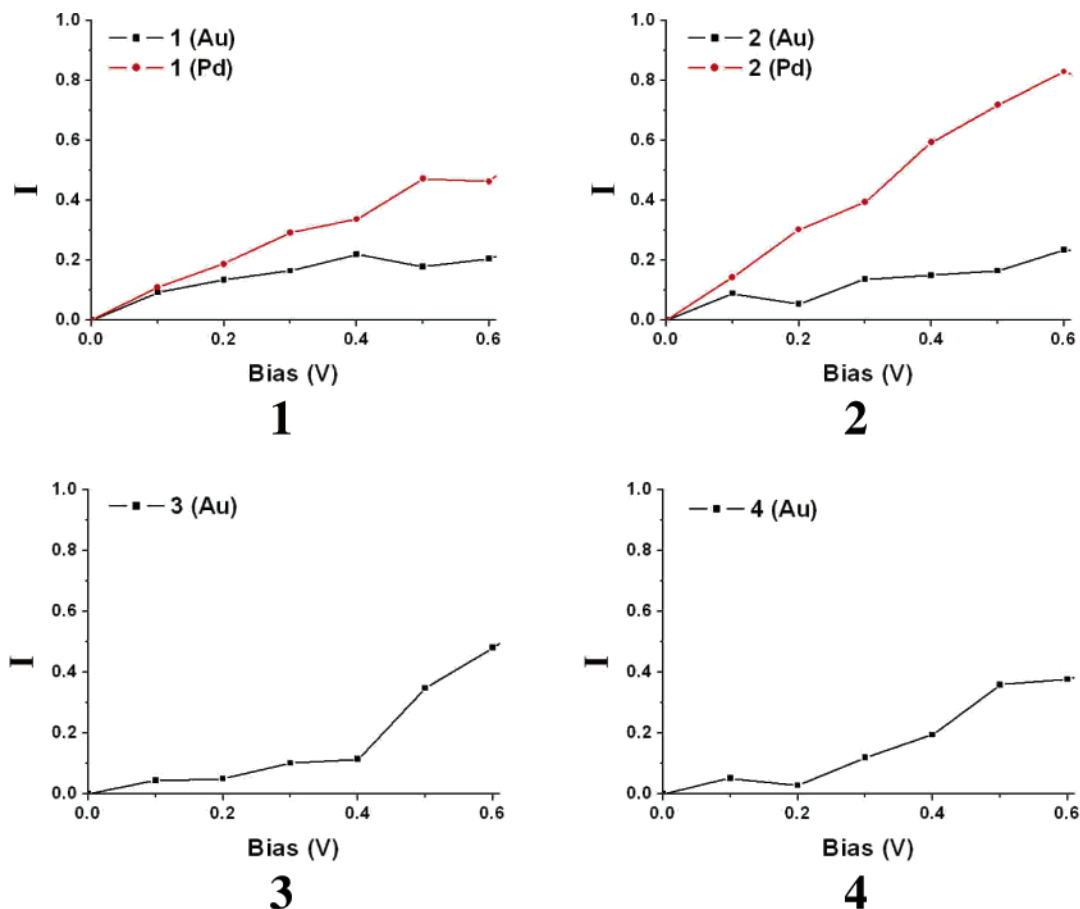


**Figure 6.** *I*–*V* characteristics of all of the Au- and Pd-contacted systems (1–4) investigated in this study.

configuration of the contact geometry and the possible effect of the oxidized electrode have to be carefully investigated with regard to the contact resistance.

With this general comment in mind, we now discuss Figure 6. In the low-bias regime ( $<0.1$  V), the  $I$ - $V$  behavior is nearly the same for both the gold- and palladium-contacted molecules. However, with increasing voltage, the palladium-contacted **1** and **2** exhibit consistently larger current levels at a given  $V$ , compared to the gold-contacted case. The changes in the electrode orientations and the electrode contact with the molecule do not yield significant improvement in the  $I$ - $V$  characteristics of the gold-contacted systems (**3** and **4**). The calculated  $I$ - $V$  behavior can be explained in relation to the transmission and DOS curves in Figures 3 and 5. When the bias is applied, the chemical potential or Fermi level of one of the electrodes is lowered below the HOMO level, thereby inducing emission of electrons from the HOMO level into the electrode. The resulting loss of electrons from the HOMO level is filled by electrons from the other electrode, and steady-state current ensues. The current level in this case is mainly determined by the HOMO density of states (DOS), in particular, the DOS at the tip of the electrode atoms in the range of biases considered (Figure 5). The larger and broader DOS of the HOMO, together with broader transmission characteristics (Figure 3), renders the current level higher in the palladium-contacted system. For larger bias voltages, the electrons in LUMO would start contributing to the current. In this case, the palladium-contacted molecule would exhibit even higher conductance because of its smaller  $E_F$ - $E_{\text{LUMO}}$  gap, compared to that of the gold-contacted molecule. However, in the presence of an external electric field, both the HOMO-LUMO and  $E_F$ - $E_{\text{LUMO}}$  gaps could be sensitively affected, the investigation of which would shed further insight to the problem. In fact, it might be possible that the LUMO would start playing a role at a much lower bias.

## Conclusion

We have shown in this work that the enhanced conductance of the palladium-contacted **1** and **2** is due to (i) enhanced coupling with the molecule, (ii) improved electron delocalization at the center of the molecule, and (iii) decreased gap between the Fermi level ( $E_F$ ) and the conductance peak associated with the LUMO. These findings indicate that the palladium is a better electrode, even though it has a work function nearly identical to that of gold atom. This observation is consistent with previous work on the transmission of palladium-contacted benzenedithiol.<sup>9</sup> Earlier attempts at improving conductance characteristics of isolated molecules or improving charge injection at interfaces included changing the characteristics of the molecule by derivatization.<sup>16</sup> The present work demonstrates that changing the chemical nature of the electrode can be an efficient and alternative way of improving the nature of the metal-molecule contact. Needless to say, much experimental work needs to be done in terms of molecular device fabrication and  $I$ - $V$  characterization, using palladium contacts. Substantial progress in this direction has been made in the fabrication and measurement of palladium-contacted carbon nanotubes.<sup>31</sup> On the theoretical front, it would be worthwhile to examine the effect of an oxidized electrode on the  $I$ - $V$  characteristics of these electrode-molecule systems.

**Acknowledgment.** P.T. and D.M.K. acknowledge support from KISTI (Korea Institute of Science and Technology Information) under the "Grand Challenge Support Program" with Dr. Sang Min Lee as the technical supporter. The use of

the computing system of the Supercomputing Center is also greatly appreciated.

## References and Notes

- (1) Dadosh, T.; Gordin, Y.; Krahne, R.; Khivrich, I.; Mahalu, D.; Frydman, V.; Sperling, J.; Yacoby, A.; Bar-Joseph, I. *Nature* **2005**, *436*, 677.
- (2) Nitzan, A.; Ratner, M. A. *Science* **2003**, *300*, 1384.
- (3) Heath, J. R.; Ratner, M. A. *Phys. Today* **2003**, *56* (5), 43.
- (4) Carroll, R. L.; Gorman, C. *Angew. Chem., Int. Ed.* **2002**, *41*, 4378.
- (5) Piva, P. G.; DiLabio, G. A.; Pitters, J. L.; Zikovsky, J.; Rezek, M.; Dogel, S.; Hofer, W. A.; Wolkow, R. A. *Nature* **2005**, *435*, 658.
- (6) Gonzalez, C.; Simón-Manso, Y.; Batteas, J.; Marquez, M.; Ratner, M.; Mujica, V. *J. Phys. Chem. B* **2004**, *108*, 18414.
- (7) Basch, H.; Ratner, M. A. *J. Chem. Phys.* **2003**, *119*, 11926. Basch, H.; Ratner, M. A. *J. Chem. Phys.* **2003**, *119*, 11943.
- (8) Basch, H.; Cohen, R.; Ratner, M. A. *Nano Lett.* **2005**, *5*, 1668.
- (9) Seminario, J. M.; De La Cruz, C. E.; Derosa, P. A. *J. Am. Chem. Soc.* **2001**, *123*, 5616.
- (10) Palacios, J. J.; Pérez-Jiménez, A. J.; Louis, E.; Vergés, J. A. *Phys. Rev. B* **2001**, *64*, 115411.
- (11) Xue, Y.; Datta, S.; Ratner, M. A. *J. Chem. Phys.* **2001**, *115*, 4292.
- (12) Green, M. L. H.; Marder, S. R.; Thompson, M. E.; Bandy, J. A.; Bloor, D.; Kolinsky, P. V.; Jones, R. J. *Nature* **1987**, *330*, 360. Kanis, D. R.; Ratner, M. A.; Marks, T. J. *Chem. Rev.* **1994**, *94*, 195. Dalton, L. R. *J. Phys. Condens. Matter* **2003**, *15*, R897.
- (13) Long, N. J. *Angew. Chem., Int. Ed. Engl.* **1995**, *34*, 21. Whittall, I. R.; McDonagh, A. M.; Humphrey, M. G. *Adv. Organomet. Chem.* **1998**, *42*, 291. Bella, S. D. *Chem. Soc. Rev.* **2001**, *30*, 355.
- (14) Palacios, J. J.; Pérez-Jiménez, J.; Louis, E.; SanFabián, E.; Vergés, J. A. *Phys. Rev. Lett.* **2003**, *90*, 106801.
- (15) Tarakeswar, P.; Kim, D. M. *J. Phys. Chem. B* **2005**, *109*, 7601.
- (16) Karzazi, Y.; Crispin, X.; Kwon, O.; Brédas, J. L.; Cornil, J. *Chem. Phys. Lett.* **2004**, *387*, 502.
- (17) Reichert, J.; Ochs, R.; Beckmann, D.; Weber, H. B.; Mayor, M. *Phys. Rev. Lett.* **2002**, *88*, 176804.
- (18) Heurich, J.; Cuevas, J. C.; Wenzel, W.; Schön, G. *Phys. Rev. Lett.* **2002**, *88*, 256803.
- (19) McCreery, R.; Dieringer, J.; Solak, A. O.; Snyder, B.; Nowak, A. M.; McGovern, W. R.; DuVall, S. J. *Am. Chem. Soc.* **2003**, *125*, 10748; *J. Am. Chem. Soc.* **2004**, *125*, 10748. Ashwell, G. J.; Mohib, A. *J. Am. Chem. Soc.* **2005**, *127*, 16238.
- (20) Banse, B. A.; Koel, B. E. *Surf. Sci.* **1990**, *232*, 275. Bondzie, V. A.; Kleban, P.; Dwyer, D. J. *Surf. Sci.* **1996**, *347*, 319. Aggarwal, S.; Monga, A. P.; Perusse, S. R.; Ramesh, R.; Ballarotto, V.; Williams, E. D.; Chalamala, B. R.; Wei, Y.; Reuss, R. H. *Science* **2000**, *287*, 2235.
- (21) Frisch, M. J.; Trucks, G. W.; Schlegel, H. B.; Scuseria, G. E.; Robb, M. A.; Cheeseman, J. R.; Montgomery, J. A., Jr.; Vreven, T.; Kudin, K. N.; Burant, J. C.; Millam, J. M.; Iyengar, S. S.; Tomasi, J.; Barone, V.; Mennucci, B.; Cossi, M.; Scalmani, G.; Rega, N.; Petersson, G. A.; Nakatsuji, H.; Hada, M.; Ehara, M.; Toyota, K.; Fukuda, R.; Hasegawa, J.; Ishida, M.; Nakajima, T.; Honda, Y.; Kitao, O.; Nakai, H.; Klene, M.; Li, X.; Knox, J. E.; Hratchian, H. P.; Cross, J. B.; Bakken, V.; Adamo, C.; Jaramillo, J.; Gomperts, R.; Stratmann, R. E.; Yazyev, O.; Austin, A. J.; Cammi, R.; Pomelli, C.; Ochterski, J. W.; Ayala, P. Y.; Morokuma, K.; Voth, G. A.; Salvador, P.; Dannenberg, J. J.; Zakrzewski, V. G.; Dapprich, S.; Daniels, A. D.; Strain, M. C.; Farkas, O.; Malick, D. K.; Rabuck, A. D.; Raghavachari, K.; Foresman, J. B.; Ortiz, J. V.; Cui, Q.; Baboul, A. G.; Clifford, S.; Cioslowski, J.; Stefanov, B. B.; Liu, G.; Liashenko, A.; Piskorz, P.; Komaromi, I.; Martin, R. L.; Fox, D. J.; Keith, T.; Al-Laham, M. A.; Peng, C. Y.; Nanayakkara, A.; Challacombe, M.; Gill, P. M. W.; Johnson, B.; Chen, W.; Wong, M. W.; Gonzalez, C.; Pople, J. A. *Gaussian 03*, revision A.1; Gaussian, Inc.: Pittsburgh, PA, 2004.
- (22) Ross, R. B.; Powers, J. M.; Atashroo, T.; Ermler, W. C.; LaJohn, L. A.; Christiansen, P. A. *J. Chem. Phys.* **1990**, *93*, 6654. LaJohn, L. A.; Christiansen, P. A.; Ross, R. B.; Atashroo, T.; Ermler, W. C. *J. Chem. Phys.* **1987**, *87*, 2812.
- (23) Hay, P. J.; Wadt, W. R. *J. Chem. Phys.* **1985**, *82*, 270. Hay, P. J.; Wadt, W. R. *J. Chem. Phys.* **1985**, *82*, 299.
- (24) Louie, S. G.; Cohen, M. L. *Phys. Rev. Lett.* **1975**, *35*, 866. Chelikowsky, J. R.; Chadi, D. J.; Cohen, M. L. *Phys. Rev. B* **1981**, *23*, 4013.
- (25) Mujica, V.; Kemp, M.; Ratner, M. A. *J. Chem. Phys.* **1994**, *101*, 6849. Mujica, V.; Kemp, M.; Ratner, M. A. *J. Chem. Phys.* **1994**, *101*, 6856. Mujica, V.; Kemp, M.; Roitberg, A.; Ratner, M. A. *J. Chem. Phys.* **1996**, *104*, 7296. Ratner, M. A.; Davis, B.; Kemp, M.; Mujica, V.; Roitberg, A.; Yaliraki, S. *Ann. N.Y. Acad. Sci.* **1998**, *852*, 22.
- (26) Palacios, J. A.; Pérez-Jiménez, J.; Louis, E.; SanFabián, E.; Vergés, J. A. *Phys. Rev. B* **2002**, *66*, 035322.
- (27) Palacios, J. J.; Pérez-Jiménez, J.; Louis, E.; SanFabián, E.; Vergés, J. A.; García, Y. In *Computational Chemistry: Reviews of Current Trends*; Leszczynski, J., Ed.; World Scientific: Singapore, 2005.

- (28) Palacios, J. J. *Phys. Rev. B* **2005**, 72, 125424.
- (29) Ulrico, J.; Esrall, D.; Pontius, W.; Venkataraman, L.; Millar, D.; Doerrer, L. H. *J. Phys. Chem. B* **2006**, 110, 2462.
- (30) Paulsson, M.; Stafström, S. *Phys. Rev. B* **2001**, 64, 035416.
- (31) Javey, A.; Guo, J.; Wang, Q.; Lundstrom, M.; Dai, H. *Nature* **2003**, 424, 654.